

Swift heavy ion effects in gallium nitride

S. Mansouri^{1,*}, P. Marie¹, C. Dufour¹, G. Nouet¹, I. Monnet², H. Lebius², Z. Benamara³, Y. Al-Douri⁴

¹⁾ *Structure des Interfaces et Fonctionnalité des Couches Minces (SIFCOM), UMR CNRS*

6176, ENSICAEN, 6 Boulevard du Maréchal Juin 14050 Caen cedex, France.

²⁾ *Centre Interdisciplinaire de Recherches Ions Lasers (CIRIL), CEA-CNRS-ENSICAEN,*

BP5133 14070 Caen cedex , France.

³⁾ *Laboratoire de microélectronique appliquée université Djillali Liabbes de Sidi Bel Abbes,*

22000 – Algeria.

⁴⁾ *CRISMAT, ENSICAEN/CNRS UMR 6805, F-14050, Caen, France.*

Abstract

GaN layers were irradiated at room temperature with swift heavy ions. AFM (atomic force microscopy) images of specimens irradiated under grazing incidence show tracks. With 74 MeV Kr, the contrast is very faint unlike for 92 MeV Xe and 104 MeV Pb. This behavior indicates that the electronic energy loss threshold to produce tracks at grazing incidence is around 17keV/nm. These tracks consist of two parts, one with a rather homogeneous contrast, and a second with regularly spaced dots. Measurements in the bulk region after irradiation with 132 MeV Pb ions show tracks with a diameter of about 3 nm.

Keywords: GAN, AFM, Threshold energy.

1. Introduction

Energy deposition in materials was extensively carried out during the last two decades. Systematic investigations- have allowed analyzing the behavior of metals, insulators and semiconductors in a large electronic stopping power range thanks to heavy ions accelerated to a few hundreds of MeV. According to the intrinsic properties of the materials, different induced effects were found: latent tracks in oxides, defects in metals. Concerning the semiconductors, the electronic excitation induced by high energy heavy ion irradiation can

^{*}) For corresponding, E-mail: mansedik@yahoo.fr.

lead to different effects. For elemental semiconductors, Si and Ge, it was initially shown that recrystallized tracks were formed in amorphous materials [1]. Si and Ge single crystals displayed a very low sensitivity only to very high electronic excitations [2-5]. For compound semiconductors, some are rather insensitive (e.g. SiC, GaAs, GaP, AlN) whereas others are sensitive (InP, InSb, GaSb) [6].

Nitride semiconductors, GaN, AlN and InN, and the ternary and quaternary related compounds are materials that have attracted a lot of attention in the last few years in optoelectronic and microelectronic fields: blue light emitting diodes [7], high-temperature and high-power electronic devices [8]. Because of the lack of bulk substrates, wurtzite gallium nitride layers are usually grown by means of heteroepitaxial techniques on sapphire or SiC substrates [9]. Due to the considerable lattice mismatch between GaN and these substrates, a high density of threading dislocations (10^{10}cm^{-2}) is present. The introduction of the ELO (Epitaxial Lateral Overgrowth) technique has allowed bringing down the density of dislocations to the range of $5\times10^6\text{ cm}^{-2}$ [10]. As a consequence, Nakamura *et al.*[11] demonstrated a blue laser diode with a lifetime of more than 10 000 h.

Due to the interest in doping nitride semiconductors by rare earths in order to get specific emissions, interaction of ions with GaN was extensively studied in the last past decade. These works were mainly carried out in the elastic collision range. Recently, analysis of the damage creation was reported with swift heavy ions ($^{197}\text{Au}^{16+}$, $^{208}\text{Pb}^{27+}$) [12,13]. It was shown that tracks exhibiting a large degree of structural disordering were formed, and that damage accumulation and efficient erosion of the irradiated layer occur at low values of electronic energy deposition density (1.3keV/nm^3).

2. Experiments

In this work, we wish to improve the analysis of energy loss due to inelastic collisions in GaN mainly under grazing incidence. A $4\text{ }\mu\text{m}$ thick epilayer GaN (n-type Si doped) grown on the *c* plane of sapphire was used. The crystallographic structure corresponds to the 2H hexagonal polytype or wurtzite. The density of threading dislocations is about $5\times10^8\text{cm}^{-2}$, and the carrier concentration is $3\times10^{17}\text{cm}^{-3}$. The samples, bulk and ion-thinned, were irradiated at room temperature at the GANIL (Grand Accélérateur National d'Ions Lourds) accelerator in Caen, France with 74 MeV $^{86}\text{Kr}^{18+}$, 92 MeV $^{129}\text{Xe}^{23+}$, 104 MeV $^{209}\text{Pb}^{28+}$, and 132 MeV $^{209}\text{Pb}^{32+}$ ions provided by the beam line IRRSUD (Table 1). Due to the low fluences used no warm up of the sample was observed.

Specific data concerning the experiments are given in table 2. The ranges are larger than the thicknesses of the specimens avoiding the implantation of the ions in the material. The fluences were kept low enough to prevent the overlapping of tracks.

A fast way to characterize the specimens is to use a non-destructive technique without any preparation of the specimen; atomic force microscopy (AFM) offers this facility. However, the detection of the damages is not so easy if no swelling, hillock or crater formations occur, and atomic scale images can be required [14]. Very recently, materials were irradiated under grazing angles of incidence, in the range of (1-6°) [15,16]. The energy is now deposited in the vicinity of the surface, and therefore the damages are locally enhanced. It was shown that multiple periodically spaced dots can be created by a single ion, and that the spacing depends on the incidence angle. The efficiency and sensitivity of this experimental method being proven, it was used in our experiments on GaN to allow the detection of the first stages of damaging. The analysis by transmission electron microscopy (TEM) was only done for the most energetic ion on a normal incidence, Pb, when the tracks were most certainly formed, and their density was large enough. It was performed in a Jeol 2010 with a

field emission gun operating at 200 kV. Specimens were ion-thinned at 5 keV with argon ions before irradiation. AFM images were carried out in the tapping mode.

| Ions | 74 MeV $^{86}\text{Kr}^{18+}$ | 92 MeV $^{129}\text{Xe}^{23+}$ | 104 MeV $^{209}\text{Pb}^{28+}$ | 132 MeV $^{209}\text{Pb}^{32+}$ |
|-------------------------------|-------------------------------|--------------------------------|---------------------------------|---------------------------------|
| (dE/dx) _e (keV/nm) | 17,1 | 22.5 | 24,1 | 28.3 |
| (dE/dx) _n (keV/nm) | 0.08 | 0.20 | 0.57 | 0.47 |
| Ranges (μm) | 8.3 | 8.2 | 8.3 | 9.3 |

Table 1: Electronic, (dE/dx)_e, nuclear, (dE/dx)_n, stopping power, and ranges of swift heavy ions used in the irradiation of GaN epilayers.

| Ions | 74 MeV $^{86}\text{Kr}^{18+}$ | 92 MeV $^{129}\text{Xe}^{23+}$ | 104 MeV $^{209}\text{Pb}^{28+}$ | 132 MeV $^{209}\text{Pb}^{32+}$ |
|-------------------------------------|-------------------------------|--------------------------------|---------------------------------|---------------------------------|
| Incidence angle ($^\circ$) | 1.5 | 90 | 1.5 | 90 |
| Beam flux (ions/cm ² /s) | $4 \cdot 10^6$ | $1.5 \cdot 10^8$ | $4 \cdot 10^6$ | $1.5 \cdot 10^8$ |
| Fluence (ions/cm ²) | $5 \cdot 10^8$ | $5 \cdot 10^{10}$ | $1 \cdot 10^9$ | $5 \cdot 10^{10}$ |

Table 2: Specific data of the irradiation.

Before irradiation, the surface is formed by atomically flat terraces with atomic steps; the roughness Rms (root-mean-square) is equal to 0.15 nm. The heights of the steps correspond to c or $c/2$ ($a_{\text{GaN}} = 0.319$ nm, $c_{\text{GaN}} = 0.5185$ nm). Some dislocations are clearly visible as black spots (Fig.1b and c).

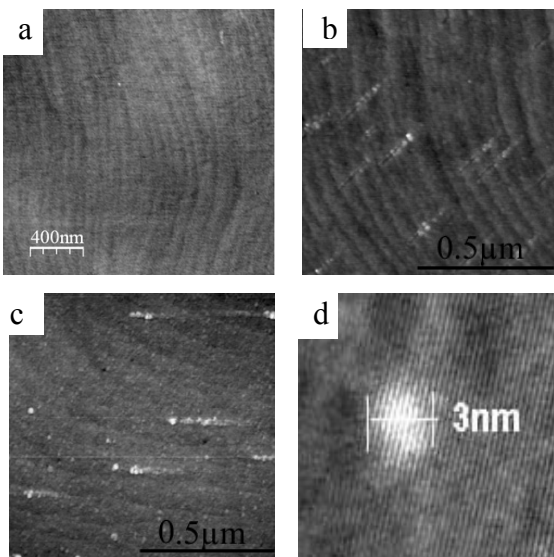


Fig. 1: AFM images after irradiation under grazing incidence: a) 74 MeV $^{86}\text{Kr}^{18+}$ very faint contrast, b) 92 MeV $^{129}\text{Xe}^{23+}$ and c) 104 MeV $^{209}\text{Pb}^{28+}$: formation of dots, d) TEM image: GaN irradiated with 132 MeV $^{209}\text{Pb}^{32+}$ under normal incidence showing tracks of 3 nm diameter.

With the 74 MeV $^{86}\text{Kr}^{18+}$ ions, irradiation leads to a slight change of the features of the surface with formation of faint tracks that makes valid the assumption of a threshold for the formation of tracks on the surface in this range of energy. More important alteration of the

surface is obtained with the two other ions with a greater electronic stopping power, 92 MeV $^{129}\text{Xe}^{23+}$ and 104 MeV $^{209}\text{Pb}^{28+}$ (Fig.1a, b and c).

The density of observed tracks is rather in agreement with the fluences: Kr 5 ions/ μm^2 : 6 impacts/ μm^2 , Xe 10 ions/ μm^2 : 8 impacts/ μm^2 , Pb 10 ions/ μm^2 : 5 impacts/ μm^2 . Assuming that one ion creates one track and using the fluence reached for a normal incidence (measured during the experiment with an accuracy of 10%) it is possible to calculate the incidence angle. In grazing incidence, the tracks are non homogeneous, and non continuous with formation of separated dots at the end of the track. For the same track, the detected features on the AFM images must be associated with events at different depths. In these conditions, the variation of the morphological characteristics of the tracks between the beginning and the end can be attributed to either surface or depth effects, and to one or several mechanisms of energy loss: surface sputtering, electronic excitation.

Dots are systematically formed with Xe and Pb ions, with Kr ions the great majority of the tracks is dot free. That indicates that the electronic energy loss threshold to produce tracks on the surface by grazing incidence irradiation is around 17 keV/nm. Other experiments, like TEM observation of normal incidence irradiated samples, are needed to know if this threshold for surface effects is the same as the threshold for track formation in bulk specimen. Such a threshold is up to now not known for GaN. Another important characteristic is the diameter of the tracks. Due to the long-reaching forces employed in AFM measurements, the measurement of the diameter of a surface structure is folded with the tip size, which is not well known. We have therefore chosen to utilize TEM measurements for the diameter of normal incidence targets. Ion-thinned TEM specimens were observed after irradiation with 132 MeV $^{209}\text{Pb}^{32+}$, and the TEM images show tracks with a diameter of about 3 nm (Fig.1d).

Considering the lengths of the tracks and the incidence angles calculated with the number of impacts, the maximal depths of the visible part of the tracks were estimated (Table 3). Due to the too faint contrast of the tracks after irradiation with Kr ions, only the irradiations with Xe and Pb ions were taken into account. The smaller the incidence angle, the larger the length is, as expected. Knowing that the diameter of the tracks is not very sensitive to the electronic stopping power, we can take this value of 3 nm for Xe and Pb ions. With such depths and diameters, the surface should not be altered, however dots with a height of 3 nm are formed.

| | 92 MeV $^{129}\text{Xe}^{23+}$ | 104 MeV $^{209}\text{Pb}^{28+}$ |
|---|--------------------------------|---------------------------------|
| Average length of the tracks (nm) | 190 | 246 |
| Incidence angle ($^\circ$) | 1.1 | 0.7 |
| Depth of the end of the visible part of the tracks (nm) | 3.7 | 2.7 |
| Height of the dots (nm) | 3 | 3 |

Table 3: Morphological features of the tracks.

These dots were also observed after irradiation of SrTiO_3 and SiO_2 [15,16], the heights being similar: 3 and 2.5 nm, respectively. The common point between these three materials irradiated with the same swift heavy ions under grazing incidence is the modification of the top surface of the layer. The AFM images show that the tracks consist of two parts, one with a rather homogeneous contrast, and the second with regularly spaced dots (Fig.1b and c). In these conditions of irradiation, the interaction of the ion with the surface should be visible as an elongated defect corresponding to the sputtering or evaporation of the material when the ion impinges the surface. The first part could be attributed to this effect. In the case of SrTiO_3 , the dots were explained on the basis of deposition of energy on the planes parallel to the surface containing the highest density of electrons [15], but this model fails for the irradiation of amorphous materials.

The deposition of discontinuous energy at the nanometric scale was then considered [16]. Although, the formation of dots is therefore still controversial, this phenomenon gives a new option to the nanostructuration of the surface of semiconductors.

4. Conclusion

This paper offers the opportunity to characterize the effect of a 74 MeV Kr, 92 MeV Xe and 104 MeV Pb swift heavy ion impinging at normal and grazing incidence on GaN. In figure 1 we show AFM and TEM images of a sample that was irradiated under grazing and normal incidence angles resulting in two types of defects. the defects density observed is not important to affect the GaN properties. We conclude that GaN material is the less sensitive to heavy ions irradiations compared to the classical semiconductors like Si, Ge and GaAs. This makes it the appropriate material for applications in hostile's environments and in panel solar technologies.

Acknowledgements

Authors thank LUMILOG (www.lumilog.com) for providing GaN material and the support of the EU Marie Curie RTN contract MRTN-CT-2004-005583 (PARSEM)

References

- [1] K. Izui, S. Furuno, *Proc. XIth International Congress on Electron Microscopy* (Kyoto, pp. 1299, 1986)
- [2] M. Toulemonde, J. Dural, G. Nouet, P. Mary, J. F. Hamet, M. F. Beaufort, J. C. Desoyer, C. Blanchard, J. Auleytner, *phys. stat. sol. (a)* **114**, 467 (1989)
- [3] A. Colder, M. Levalois, P. Marie, *Eur. Phys. J. AP* **13**, 89 (2001)
- [4] A. Dunlop, G. Jaskierowicz, S. Della-Negra, *Nucl. Instr. and Meth. B* **146**, 296 (1998)
- [5] A. Colder, O. Marty, B. Canut, M. Levalois, P. Marie, X. Portier, S. M. M. Ramos, M. Toulemonde, *Nucl. Instr. and Meth. B* **174**, 471 (2001)
- [6] S. Dhamodaran, A. P. Pathak, A. Dunlop, G. Jaskierowicz, S. Della-Negra, *Nucl. Instr. and Meth. B* **256**, 229 (2007)
- [7] J. W. Orton, C. T. Foxton, *Rep. Prog. Phys.* **61**, 1 (1998)
- [8] H. Morkoç, R. Cingolani, W. Lambrecht, B. Gil, H. X. Jiang, J. Lin, D. Pavlidis, K. Shenai, *MRS Internet J. Nitride Semicond. Res.* **4S1**, G1.2 (1999)
- [9] S. C. Jain, M. Willander, J. Narayan, R. Van Overstraeten, *J. Appl. Phys.* **87**, 965 (2000)
- [10] P. Gibart, B. Beaumont, P. Vennegues, “in *Nitride Semiconductors, Handbook on Materials and Devices*”, edited by P. Ruterana, M. Albrecht, J. Neugebauer (Wiley, pp.45, 2003)
- [11] S. Nakamura, M. Senoh, S. Nagahama, N. Iwasa, T. Yamada, T. Matsushita, H. Kiyoku, Y. Sugimoto, T. Kozaki, H. Umemoto, M. Sano, K. Chocho, *Proc. International Conference on Nitride Semiconductors S-1*, 444 (1997)
- [12] S. O. Kucheyev, H. Timmers, J. Zou, J. S. Williams, J. Jacadish, G. Li, *J. Appl. Phys.* **95**, 5360 (2004)
- [13] C. H. Zang, Y. Song, Y. M. Sun, H. Chen, Y. T. Yang, L. H. Zhou, Y. F. Jin, *Nucl. Instr. and Meth. B* **256**, 199 (2007)
- [14] J. Liu, H. J. Yao, Y. M. Sun, J. L. Duan, M. D. Hou, D. Mo, Z. G. Wang, Y. F. Jin, H. Abe, Z. C. Li, N. Sekimura, *Nucl. Instr. and Meth. B* **245**, 126 (2006)

- [15] E. Akcöltekin, T. Peters, R. Meyer, A. Duvenbeck, M. Klusmann, I. Monnet, H. Lebius, M. Schleberger, *Nature Nanotechnology* **2**, 290 (2007)
- [16] A. M. J. F. Carvalho, M. Marinoni, A. D. Touboul, C. Guasch, H. Lebius, M. Ramonda, J. Bonnet, F. Saigne, *Appl. Phys.Lett.* **90**, 073116 (2007)